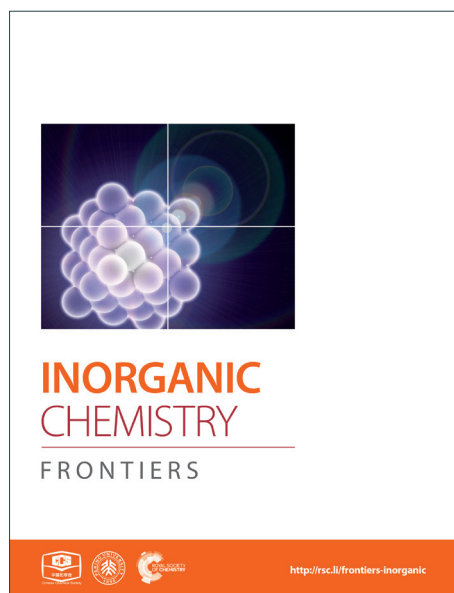
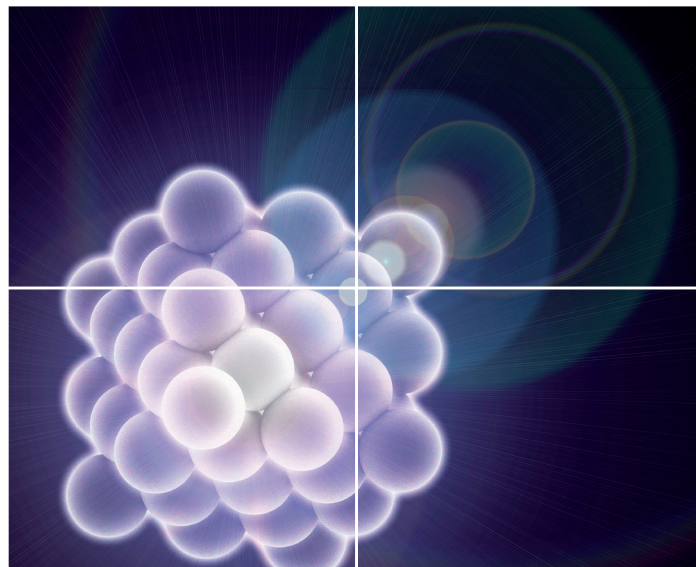


INORGANIC CHEMISTRY

FRONTIERS

Accepted Manuscript



This is an *Accepted Manuscript*, which has been through the Royal Society of Chemistry peer review process and has been accepted for publication.

Accepted Manuscripts are published online shortly after acceptance, before technical editing, formatting and proof reading. Using this free service, authors can make their results available to the community, in citable form, before we publish the edited article. We will replace this *Accepted Manuscript* with the edited and formatted *Advance Article* as soon as it is available.

You can find more information about *Accepted Manuscripts* in the [Information for Authors](#).

Please note that technical editing may introduce minor changes to the text and/or graphics, which may alter content. The journal's standard [Terms & Conditions](#) and the [Ethical guidelines](#) still apply. In no event shall the Royal Society of Chemistry be held responsible for any errors or omissions in this *Accepted Manuscript* or any consequences arising from the use of any information it contains.

ARTICLE

Synthesis, characterisation, water adsorption and proton conductivity of three Cd(II) based luminescent metal-organic frameworks

Cite this: DOI: 10.1039/x0xx00000x

Srinivasulu Parshamoni, Himanshu Sekhar Jena, Suresh Sanda and Sanjit Konar*

Received 00th January 2014,

Accepted 00th January 2014

DOI: 10.1039/x0xx00000x

www.rsc.org/

Three hydrogen bonded three dimensional (3D) Metal Organic Frameworks (MOFs) namely, [Cd(L-tart)(bpy)(H₂O)]_n·9n(H₂O) (**1**), [Cd(D-tart)(bpy)(H₂O)]_n·9n(H₂O) (**2**) and [Cd(DL-tart)(bpy)(H₂O)]_n·6n(H₂O) (**3**) (tart = tartaric acid, bpy = 4,4-bipyridine) have been synthesized by solvent diffusion technique at room temperature. Compounds **1** and **2** have been characterized by single crystal X-ray analysis whereas the powder X-ray diffraction patterns analysis shows that structural integrity of compound **3** is similar to **1** and **2**. Structural analysis of **1** and **2** shows H-bonded homochiral 3D MOFs, fabricated by the hydrogen bonded interactions between the nearby 2D pillared-layer framework through the metal-bound water, metal-bound carboxylate, free carboxylic acid and hydroxy group of L-/D- tart. The absolute configuration of all the compounds were investigated by solid state circular dichroism (CD) spectroscopy which signifies that **1** and **2** are enantiomers whereas **3** is a racemic one. The adsorption studies reveals that compounds **1-3** show significant amount of uptake for water vapor (~239 mL g⁻¹ for **1**, ~240 mL g⁻¹ in **2**, whereas 184 mL g⁻¹ for **3** at P/Po ≈ 1 bar) over other solvents (MeOH, EtOH) and an impedance measurement indicates that these compounds show proton conduction (1.3 × 10⁻⁶ S cm⁻¹ in **1**, 1.3 × 10⁻⁶ S cm⁻¹ in **2** and 4.5 × 10⁻⁷ S cm⁻¹ in **3**) at higher temperature (358 K) and at 95 % relative humidity. The observed conductivity is explained by so-called vehicle mechanism (activation energy (E_a) = 0.63-0.77 eV). Since all the compounds contain (H₃O)⁺ cations in the interlayer space, the hydronium ions might act as vehicle to transport the protons in the interlayer space. The photoluminescence properties of all the compounds are also reported.

Introduction

In the past few decades, metal-organic frameworks (MOFs) have witnessed explosive growth. Many scientific research groups have devoted to various aspects of MOFs and exploring their applications in many fields, such as gas storage/separation,¹ conductivity,² luminescence,³ catalysis,⁴ etc. Recently, chiral MOFs have also received emerging interest not only because of their aesthetically structural architectures and topologies but also their potential applications in enantioselective catalysis,⁵ chiral separation⁶ and nonlinear optics.⁷ Generally, two main approaches have been inspected for the construction of chiral MOFs; one is based on the use of chiral sources (chiral organic linkers or metal complexes), while the other is spontaneous resolution of achiral sources. Although some chiral MOFs using achiral ligands have been reported,^{6,8} construction of chiral MOFs with enantiopure ligands seem to be a straightforward but always suffers from complex synthesis and structure limitations of enantiopure ligands.⁹ In this context, using π -conjugated, rigid organic linkers with an enantiopure carboxylates is an effective

approach to synthesize homochiral MOFs where chirality is based on the ligand. Although various strategies have been documented for the synthesis of pillared-layer 3D networks, a few H-bonded pillared-layer homochiral 3D networks have been reported so far.¹⁰

Recently, the development of new materials which show proton conduction is becoming particularly important because of their potential applications in solid-state electrochemical devices such as batteries and fuel cells.¹¹ Although Nafion is a well-known proton conductor,¹² at higher temperatures (>80 °C) its performance decreases due to dehydration.¹³ In this context, several groups have dedicated their efforts to study various aspects of proton conductivity in MOFs as well as coordination polymers (CPs) and to explore their possible applications in fuel cell as an alternative to Nafion.¹⁴ In general, to show proton conduction in a material needs proton carriers such as H₃O⁺ or H⁺ given by acid or OH groups or by incorporation of proton carriers such as imidazole, triazoles, ammonium ions, hydroxonium ions, etc.¹⁵ inside the frameworks. Amongst the reported MOFs only a very few show conductivity at high temperature (80 °C and 98% RH).¹⁶ On the other hand only few

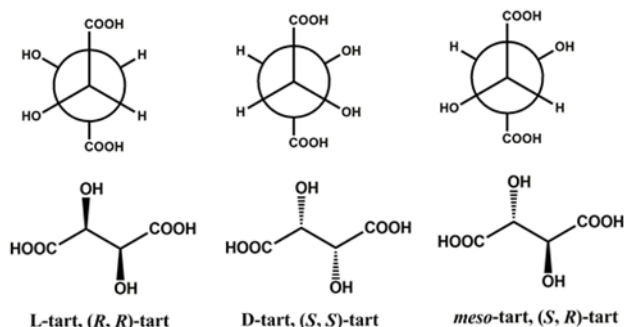
chiral MOFs exhibiting proton conducting properties are reported¹⁷ and only one of them is claimed to be a multifunctional luminescent and proton-conducting as reported by Cabeza et al.¹⁸

In the present work, we report a series of three Cd(II) based H-bonded 3D MOFs namely; [Cd(L-tart)(bpy)(H₂O)_n 9n(H₂O)] (**1**), [Cd(D-tart)(bpy)(H₂O)_n 9n(H₂O)] (**2**) and [Cd(DL-tart)(bpy)(H₂O)_n 6n(H₂O)] (**3**) by using mixture of L-, D-, DL-tartaric acid (H₂tart) and 4,4-bipyridine (bpy) ligands, obtained by slow crystallization at ambient conditions. All the three compounds are characterized by Single crystal X-ray diffraction analysis (SXRD), powder X-ray diffraction analysis (PXRD), thermo gravimetric analysis (TGA), circular dichroism (CD) study. The most remarkable characteristics of these compounds are that they show photo luminescent properties at room temperature and proton conductivity at higher temperature (85 °C) and 95% RH.

Results and discussions

Synthetic aspects

Tartaric acid played an important role in the discovery of chemical chirality and form discrete chiral complexes, MOFs and CPs with diverse functional properties depending on the metal ions used. The hydroxyl groups present in its backbone assists to shorten the distance between the metal centers and also supports in complexation. Besides that shorter distance creates a dense or rigid arrangement of metal centers in the system which might causes photoluminescence properties in d¹⁰ system.¹⁹ However the introduction of different pyridyl linkers along with tartrate acid can causes flexibility into the framework and influences their associated properties.



Scheme 1. The various tart isomers. Top: Newman projection, bottom: stereochemical drawing.

In this context, herein three compounds namely, [Cd(L-tart)(bpy)(H₂O)_n 9n(H₂O)] (**1**), [Cd(D-tart)(bpy)(H₂O)_n 9n(H₂O)] (**2**) and [Cd(DL-tart)(bpy)(H₂O)_n 6n(H₂O)] (**3**) have been synthesized by using corresponding sodium salt of tartaric acid, bpy and Cd(NO₃)₂ 4H₂O in 1:1:1 ratio through solvent diffusion technique using an ethanol/water (1:1:1) solvent system at room temperature.

Compounds **1** and **2** have been characterized by single crystal X-ray diffraction and are found to be isostructural in nature. However, we could not able to obtain diffraction quality single

crystals for compound **3** even after several attempts. In order to confirm the structural integrity of **3**, the bulk-phase powder X-ray diffraction patterns (PXRD) of the three compounds were measured and found to be in good agreement with each other which reflects that compound **3** is isostructural with **1** and **2** (Fig. 1). Furthermore, the PXRD patterns are matched well with the simulated patterns of the single crystal data of both **1** and **2**, indicating the phase purity of bulk samples. The differences in intensities of experimental PXRD with the simulated may be due to the preferred orientation of the crystalline powder sample. The observed difference peak at 2θ = 24° in Figure 1d in comparison to 1b and 1c is because two peaks are merged to a one broad peak. Additionally we have indexed the powder pattern of compound **3** using the program DICVOL91 that suggest a monoclinic crystal system with unit cell parameters, a = 11.28 Å, b = 11.67 Å, c = 8.24 Å and β = 114.622°.

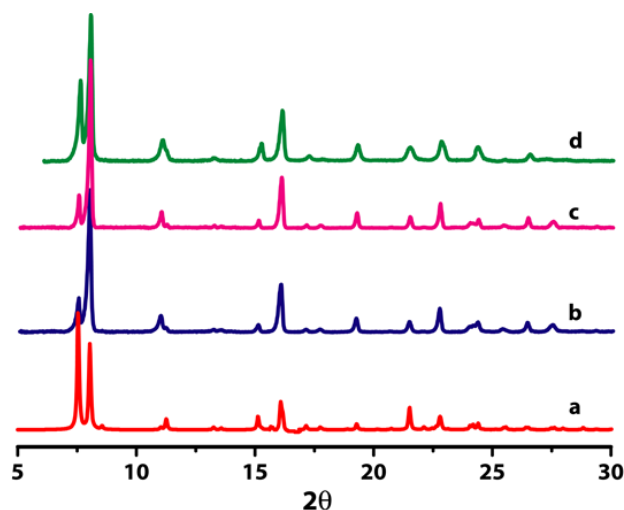


Fig. 1 PXRD patterns of compounds 1 - 3. (a) simulated PXRD of 1 (red); (b) as synthesized samples of compounds 1 and (c) compound 2; (d) as synthesized of compound 3, this matches well with compounds 1 and 2.

Compounds **1-3** show similar type of FT-IR spectra (Fig. S1) and bands are given in Table S1. A broad band was observed in the region of 3376–3400 cm⁻¹, specifies the presence of free or coordinated water molecules. The characteristic bands for the asymmetric ($\nu(\text{COO})_{\text{asym}}$) and symmetric stretching vibrations ($\nu(\text{COO})_{\text{sym}}$) of the carboxylate groups appear at 1599 – 1385 cm⁻¹ in **1**, 1605 – 1385 cm⁻¹ in **2**, and 1612 – 1392 cm⁻¹ in **3** respectively. The noted difference ($\Delta\nu = \nu(\text{COO})_{\text{asym}} - \nu(\text{COO})_{\text{sym}}$) in the bridging modes of carboxylates groups may confirm the bridging mode of the carboxylate groups found in these compounds.²⁰ The band at 1670 cm⁻¹ may be assigned to the uncoordinated and deprotonated carboxylate group of tart involved in strong hydrogen bonds.

Structural description of compounds 1 and 2

Single crystal X-ray diffraction analysis reveals that compounds **1** and **2** are isostructural and also are enantiomers. Hence only the structure of compound **1** will be discussed in

detail with a suitable comparison with **2**. The compound **1** crystallizes in the chiral orthorhombic system with space group $P2_12_12_1$. Its asymmetric unit comprises of one Cd(II) ion, one L-tart, one bpy and one coordinate water molecule (Fig. S2). Each Cd(II) centre adapts hepta coordinated with contributions from three oxygen atoms (O1, O1A and O3A) of two different L-tart ligands, one hydroxyl group (O2) of L-tart ligand, two nitrogen atoms (N1 and N2) from two different bpy linkers and one oxygen atom (O7) from water molecule and consequently a distorted pentagonal bipyramidal geometry (Fig. S3).

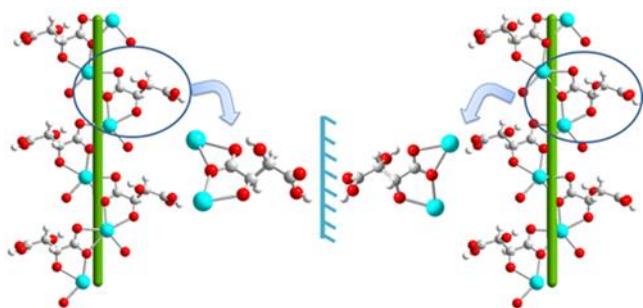


Fig. 2 Illustration of *P*-helical motifs of **1** (right) and **2** (left) running down the *b*-axis. Color code: carbon (light gray), hydrogen (gray), nitrogen (blue), oxygen (red) and cadmium (cyan).

It was found that the oxygen atoms of carboxylate group as well as hydroxyl group of L-tart and coordinated water molecules are located in equatorial plane whereas the nitrogen atoms of neutral bpy linkers are occupied in the axial positions. The Cd-O bond lengths are found to be in the range of 2.265(4) Å - 2.495(3) Å and Cd-N bond lengths are measured in the range of 2.316(5) - 2.325(5) Å. The O-Cd-O and N-Cd-N bond angles are laying in the range of 53.1(1) - 176.9(2)°. In **1** and **2**, a distinctive bridging mode of L-tart was observed which were not documented earlier in tartrate based 3d metal complexes system. Precisely, in both **1** and **2**, out of two hydroxyl and two carboxylate groups of L/D-tart, one hydroxyl and one carboxylate group coordinates to the Cd(II) centre whereas the other two remains un-coordinated. The carboxylate oxygen atoms (O1, O3) of L/D-tart coordinates to the Cd(II) centres in μ -1,1,2-fashion with a Harris notation^{21,20} of 3.21. Notable one carboxylate oxygen atom (O1) of L/D-tart bridges two Cd(II) centres in chelating bridging mode at a distance 4.60(4) Å and subtends at an angle of 146.6(1)° (Cd1-O1-Cd1A). Such bridging mode of carboxylate oxygen extends the hepta coordinated Cd(II) centres along *b* direction to form a homochiral 1D chain (*P*-helical) with a pitch of 8.406 Å (Fig. 2). It was observed that in **1** the L-tart ligands (D-tart for **2**) are arranged alternatively around the helical strand. Similarly each neutral pillared bpy linker coordinates to two Cd(II) centre at a distance of 11.72(1) Å and extends along *c* direction to form another infinite 1D chain. The aforementioned two 1D chains are perpendicularly interconnected along *bc* plane to form homochiral 2D pillared-layer framework. The resulted 2D framework encompasses continuous rectangular channels of dimensions 4.6 x 11.7 Å² (Fig. 3). The channels are supported

by weak $\pi \cdots \pi$ stacking interaction ($cg \cdots cg = 4.552$ Å) between pyridine-pyridine moieties of bpy linkers. Interestingly, the coordinated water molecules exhibit bi-furcate H-bonding interaction (2.686(5) - 2.978(9) Å) with oxygen atoms of coordinated and free carboxylate groups of L/D-tart. The oxygen atoms of the free carboxylate group also H-bonded with the hydroxyl group of L/D-tart. The H-bond parameters are listed in Table S2 and S3.

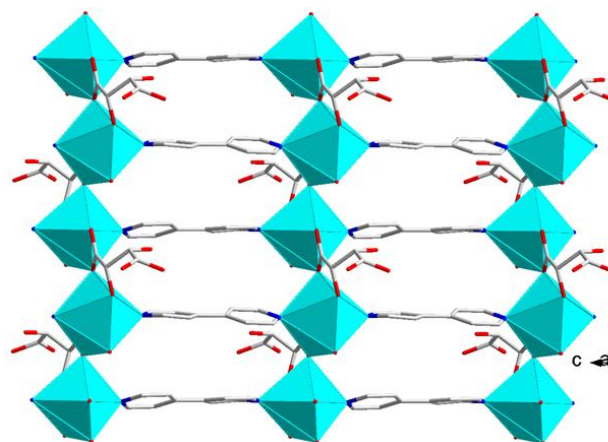


Fig. 3 Illustrations of 2D pillared layer frameworks present in **1** along the *bc*-plane. Color code; same as in Fig. 2.

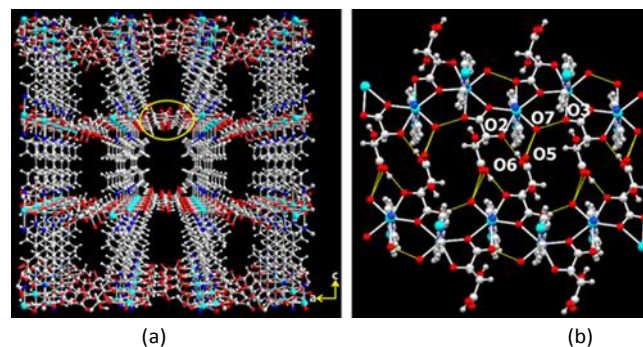


Fig. 4 Illustrations of (a) H-bonded homochiral 3D MOF found in **1**, (b) H-bonded interactions between metal-bound water and carboxylate groups with free hydroxyl and carboxylate group of L/D-tart. Color code; same as in Fig. 2.

The 3D packing analysis reveals that the above noted 2D pillared layer frameworks are H-bonded with each other to form 3D H-bonded supramolecular framework (Fig. 4 (a)). Precisely in the H-bonded networks (Fig. 4 (b)), metal-bound water molecules act as proton donors (O7) and the metal-bound carboxylate oxygen (O3) and hydroxyl group of L/D-tart as acceptors (O2), however the oxygen atoms of free carboxylic acid group of tart ligands act both donor (O6) and acceptor (O5). The noted 3D supramolecular framework enclosed with large square shaped channels (9.9 Å² x 11.5 Å²) along the *ac*-plane which are occupied by guest water molecules. It is interesting to compare the 3D packing in both the compounds (Fig. 5), the bpy pillared linker extend perpendicularly to the [Cd-(L-tart)]_n chain (Fig. 5 (a)) whereas in **2**, they arranged in “helical fashion”. Careful analysis of the homochiral 3D

supramolecular network of compound **2**, revealed that $[\text{Cd}(\text{D-tart})]_n$ acts as a rod to the helical strand (Fig. 5(b)).

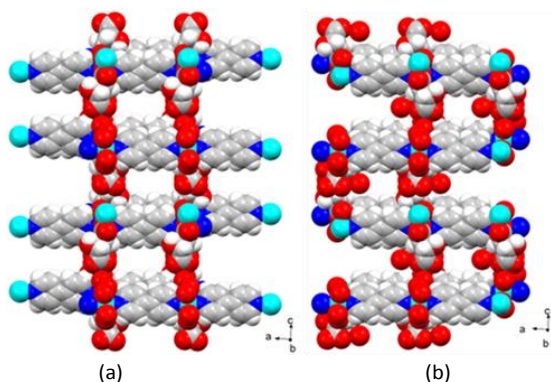


Fig. 5 Space-filling diagram of (a) compound **1** and (b) compound **2**. Colour code; same as in Fig. 2.

Topological perception of **1** reveals that, both the L-tart ligand and bpy linker are linked to two Cd(II) centers and hence can be regarded as two connected nodes. Each Cd(II) are linked to nearby four Cd(II) centres by two L-tart ligands and two bpy linkers. Therefore, the 2D homochiral porous framework can be simplified as a 4-connected uninodal net with a point symbol of $\{4^4.6^2\}$ exhibiting a *sql/Shubnikov tetragonal plane net* topology²² (Fig. S4). PLATON analysis reveals that the compound **1** contains effective free void volume of about 30.8% of the crystal volume (666.8 \AA^3 out of the 2165.5 \AA^3 unit-cell volumes). Nine highly disordered water molecules per formula unit found within the channels and that were modelled with the SQUEEZE routine in PLATON.

Circular Dichroism Study

In order to confirm the absolute configuration, compounds **1-3** were subjected for solid state circular dichroism (CD) spectroscopy. As shown in Fig. 6.

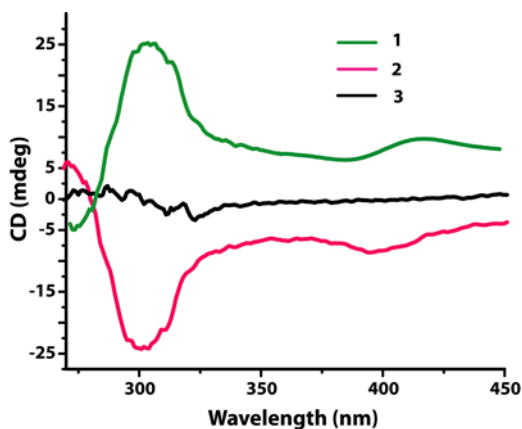


Fig. 6 Solid-state CD spectra of compounds **1**, **2**, and **3**.

Compounds **1** and **2** display positive and negative dichroic signal at wavelength range 270 -340 nm respectively and are also mirror images to each other. This signifies that they are

enantiomers. Similar analysis for compound **3** does not show any dichroic signal in the noted wavelength range which signifies the presence racemic mixtures of tartrate.

These phenomena imply that the observed homochirality in compounds **1** and **2** was transferred from the corresponding chiral tartarate ligand to the metal center and in turn to the whole framework system.

Thermal Stabilities

To examine the thermal stability of compounds **1-3**, thermo gravimetric analysis (TGA) was performed in the temperature range of 30 - 650 °C under N_2 flow with a heating rate of $10 \text{ }^\circ\text{C min}^{-1}$. Compound **1** and **2** shows similar type of profile (Fig. S5 and Fig. S6). A weight loss of 18% (Calcd. 17%) observed in the range of 75 - 180 °C which can be assigned to the loss of one coordinated water and nine lattice water molecules. The dehydrated framework was stable up to 300 °C followed by rapid weight loss due to the decomposition of the framework. Compound **3** shows a gradual weight-loss of 13% (calcd. 12%) at around 75 - 180 °C, which corresponds to the loss of one coordinate water and six lattice water molecules and the dehydrated framework stable up to 300 °C (Fig. S7).

Adsorption Studies

To examine the porous nature of all compounds, we have carried out the adsorption studies with CO_2 as well as with different solvent vapors (H_2O , EtOH and MeOH). The sorption isotherm of CO_2 at 195 K reveals very less uptake ($8 \text{ cm}^3 \text{ g}^{-1}$ in **1** and **2**, $7 \text{ cm}^3 \text{ g}^{-1}$ in **3**) signifying nonporous nature of all compounds (Fig. S8, Fig. S9 and Fig. S10). This may be due to presence of smaller channel size compare to kinetic diameter of CO_2 (kinetic diameter, 3.4 \AA).²³ However, quite interesting results were obtained with solvent vapour adsorption study.

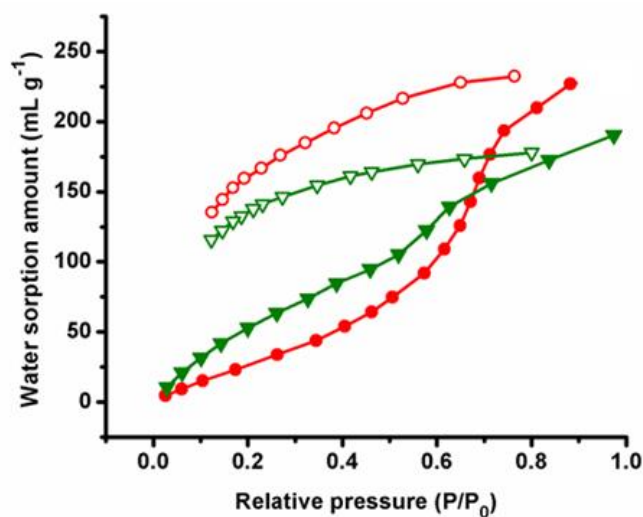


Fig. 7 Water vapour adsorption isotherm of compounds **1** (red) and **3** (green).

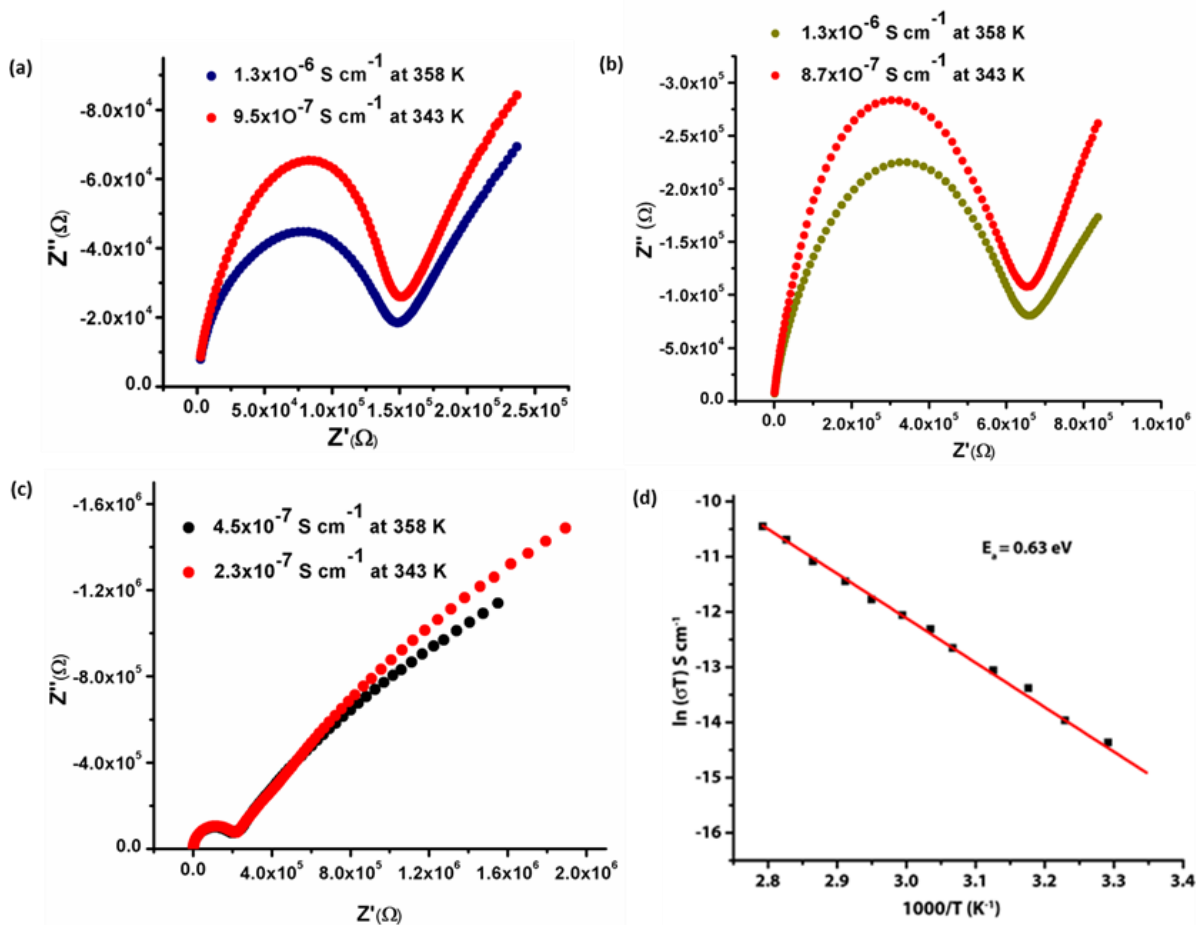


Fig. 8 The Nyquist plots for proton conductivity of (a) compound **1**, (b) compound **2**, (c) compound **3** at different temperature. (d) Arrhenius plot of activation energy for compound **1** showing activation energy value of 0.63 eV.

Adsorption isotherms of H_2O for both compounds **1** and **2** show less uptake (74 mL g^{-1}) up to ($P/P_0 \sim 0.50$) and it starts rising sharply at $P/P_0 \sim 0.63$ and reaches a final uptake volume of $\sim 239 \text{ mL g}^{-1}$ at $P/P_0 \approx 1$ bar pressure, which is comparable value with the eminent proton conducting MOFs [Me-FeCr(ox) $_3$] ($268 \text{ cm}^3 \text{ g}^{-1}$ at STP). Whereas compound **3** shows almost a linear uptake with the uptake amount of 184 mL g^{-1} at $P/P_0 \approx 1$ bar pressure (Fig. 7 and Fig. S11). Adsorption data of **1** and **2** indicates uptake of 9.3 H_2O molecules per formula unit whereas it is 7.3 in case of **3**. The low uptake in all compounds in low pressure region might be due to the difficulty in occlusion of H_2O molecules in small 2D rectangular channels and sharp uptake indicates re-accumulation of H_2O molecules inside the 3D supramolecular pore and filling of unsaturated Cd(II) centers.²⁴ Desorption isotherms of all compounds do not

retrace the adsorption profile and show large hysteresis suggest the strong interaction (H-bonding) with the pendent carboxylate oxygen atoms of the pore surface.^{23a} It is worthy to mention that the adsorption isotherms of MeOH and EtOH for all compounds show Type-III profile with the uptake amount of 31 mL g^{-1} and 23 mL g^{-1} in **1** and **2** (Fig. S12 and Fig. S13), 29 mL g^{-1} and 28 mL g^{-1} in **3** at 1 bar pressure respectively (Fig. S14). The less adsorption can be justified by correlating of their large molecular diameter of MeOH (Kinetic diameter 3.8 \AA) and EtOH (Kinetic diameter 4.3 \AA) compare to the effective pore size and unlikely to go inside into the pores, which results only surface adsorption.²⁵

Proton Conductivity Study

Although we were unable to identify the disordered water molecules in the framework from X-Ray data, but, in the TG analysis it has been observed that compounds **1** and **2** contain nine and compound **3** contains six lattice water molecules respectively. It is noteworthy to mention that in the frameworks of compounds **1** and **2**, the free acidic carboxylates and acidic metal-bound water molecules are orientated towards the interlayer space between the 2D pillared-layer frameworks (Fig. 4(b)). This observation encouraged us to evaluate their proton conductivity properties.

We have evaluated the proton conductivity of all compounds **1-3** by ac impedance analysis. All the compounds were exposed and equilibrated at relative humidity for 24 h before measurement. The proton conductivity of all compounds was estimated from the Nyquist plots as shown in Fig. S15, S16 and S17. Compounds **1-3** show proton conductivity values of $5.0 \times 10^{-10} \text{ S cm}^{-1}$ for **1**, $5.2 \times 10^{-10} \text{ S cm}^{-1}$ for **2** and $1.3 \times 10^{-10} \text{ S cm}^{-1}$ for **3** at 298 K and 95% relative humidity (RH). In order to assess the effect of humidity on the proton conduction, we performed a humidity sweep impedance measurement and the results shows that all the compounds display better conductivity at 95% RH (Table S4). The observed distorted half-circles in the Nyquist plots might be due to the closeness of relaxation frequencies of different electro active region resulting only one distorted or depressed semicircle.²⁶

We have also performed the temperature dependent proton conductivities for all compounds at constant 95% RH which shows that the proton conductivities of all the compounds increased with increasing temperature. Compound **1** shows a wide range of proton conductivities from $1.9 \times 10^{-9} \text{ S cm}^{-1}$ (303 K) to $1.3 \times 10^{-6} \text{ S cm}^{-1}$ (358 K), compound **2** shows $1.3 \times 10^{-9} \text{ S cm}^{-1}$ (303 K) to $1.3 \times 10^{-6} \text{ S cm}^{-1}$ (358 K) and compound **3** shows $9.3 \times 10^{-10} \text{ S cm}^{-1}$ (303 K) to $4.5 \times 10^{-7} \text{ S cm}^{-1}$ (358 K) (Fig. 8). Proton conduction in MOFs, particularly at higher temperatures (more than 345 K and 98% RH) is an unusual phenomenon and there are only few reports available in the literature where MOFs containing lattice H₂O molecules, conduct protons at higher temperature (PCMOF-5: $4 \times 10^{-3} \text{ S cm}^{-1}$ at 335 K),^{16c} (MIL-53(Fe)-(NH₂)₂: $4.1 \times 10^{-8} \text{ S cm}^{-1}$ at 353 K)^{16d}, (Ca-BTC-H₂O: $3.2 \times 10^{-5} \text{ S cm}^{-1}$ at 345 K).^{16e}

To ensure the stabilities of the frameworks of all the compounds after exposing at 98% RH for 24 h at room temperature (298 K) and at 358 K, the exposed compounds are subjected to PXRD and TG analysis. The PXRD analysis of the samples **1** and **2** reveals all major peaks are well matched with as-synthesized sample except the peak at around $2\theta = 7 - 8^\circ$ (Fig. S18 and Fig. S19). It was found that the two peaks merged to a broad peak which might be due to the shift of H-bonded layers in the lattice during grinding which produces different phase than that obtained in the single crystalline form. However in case of **3** all peaks are well matched with as synthesized sample (Fig. S20). From the TG profile, we observed that sixteen water molecules are present in compounds **1** and **2** at 298 K and 95% RH. Similarly in **3**, fourteen water molecules are present in at same conditions. Hence in **1** and **2**, six and in **3**, seven additional water molecules are accumulating in the

framework at 95% RH and room temperature. However at 358 K and 95% RH, in **1** and **2** four and in **3**, three additional water molecules are accumulating in the framework (Fig. S21, Fig. S22 and Fig. S23). The less accumulation of additional water molecules at 358 K might be due to the loss of some weakly H-bonded water molecules from each framework. However, we observed a better proton conductivity of all the compounds at 358 K. The observed relative high proton conductivity at 358 K, might be due to the presence of continuous hydrogen bonding 1D array among the acidic carboxylic acid group, coordinate and lattice H₂O molecules.^{16e} Although each framework accumulates more numbers of H₂O molecules at 298 K, the less conductivity might be due to the presence of discrete H-bonded clusters in the framework. From the above study, it can be concluded that the free acidic carboxylic acid and acidic metal-bound water molecules acts as proton source and lattice water molecules carries the proton in a 1D array in the interlayer space between the 2D networks.

The activation energies for the proton migration of the materials give reasonable insight into the possible mechanism for the movement of protons in solids, i.e. whether it is Grotthuss (< 0.6 eV) or vehicular mechanism (> 0.6 eV).²⁷ In the present study, temperature dependencies of the conductivity of all the compounds were measured, and their corresponding Arrhenius plots were shown in (Fig. 8d, Fig. S24 and S25). The activation energies (E_a) for the compounds **1**, **2**, and **3** were 0.63 eV, 0.67 eV and 0.77 eV respectively by using eq 1.

$$\sigma T = \sigma_0 e^{E_a/kT} \quad (1)$$

Although the observed activation energies are found to be low but are well in the range of reported values (0.137 eV - 1.16 eV). These values are typically observed for proton conductors that follow the vehicle mechanism. Since all the compounds contains (H₃O)⁺ cations in the interlayer space of the H-bonded 3D networks, the hydronium ions act as vehicle to transport the protons in the interlayer space.²⁸

Luminescent Properties

The solid-state luminescent emission properties of L-, D- and DL-tart, bpy and compounds **1-3** were investigated at room temperature (Fig. 9).

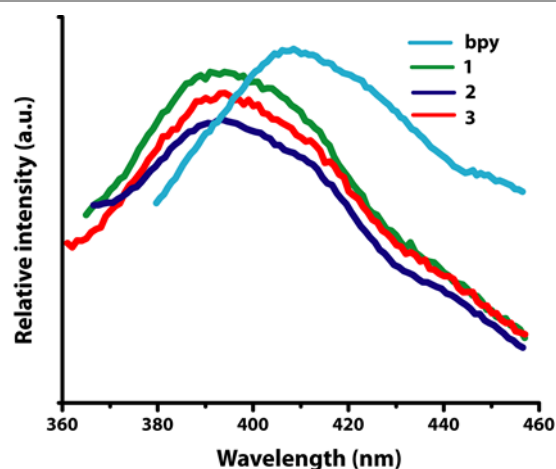


Fig. 9 Solid-state emission spectra for ligand used and compounds 1, 2, and 3.

L-, D- and DL-tart does not show any emission whereas only bpy shows stronger emission at 415 nm ($\lambda_{\text{ex}} = 321$ nm), which can be assigned to the $\pi^* \rightarrow \pi$ transitions.²⁹ Upon photo excitation, compounds 1-3 display the maximum emission peaks at 392 nm ($\lambda_{\text{ex}} = 281$ nm). The emission bands of 1-3 displays significant blue shifts, which can be attributed to the charge transfer of pyridine-based ligands to Cd(II) centers (LMCT) in comparison to the emission of bpy ligand.³⁰

CONCLUSION

We have successfully synthesised three hydrogen bonded 3D MOFs by using solvent diffusion technique at room temperature. Compounds 1 and 2 have been characterized by single crystal X-ray analysis. All three compounds were characterized by powder X-ray diffraction and thermogravimetric analysis, which shows that they are isostructural in nature. Vapour sorption studies reveals that, all compounds shows high uptake of water vapour over other solvents (MeOH, EtOH). Impedance measurement indicates that these compounds show proton conduction at higher temperature (358 K) and at 95 % relative humidity and the observed conductivity is explained by so-called vehicle mechanism (activation energy (E_a) = 0.63-0.77 eV). Since all the compounds contains (H_3O^+) cations in the interlayer space,

the hydronium ions might act as vehicle to transport the protons in the interlayer space. The photoluminescence properties of all the compounds are also reported.

EXPERIMENTAL SECTION

Materials

All the reagents and solvents for synthesis were purchased from commercial sources and used as supplied without further purification. $\text{Cd}(\text{NO}_3)_2 \cdot 6\text{H}_2\text{O}$, D-, L- and DL-tartaric acid and 4,4-bipyridine were obtained from the Sigma-Aldrich Chemical Co. India. The elemental analyses were carried out on Elementar micro vario cube elemental analyser. FT-IR spectra ($4000 - 500 \text{ cm}^{-1}$) were recorded on a KBr pellet with a Perkin Elmer Spectrum BX spectrometer. Powder X-ray diffraction (PXRD) data were collected on a PANalytical EMPYREAN instrument using Cu-K α radiation. Solid state UV-Vis spectra, luminescence spectra and CD spectra were recorded using Shimadzu UV-3101PC spectrometer, Horiba Jobin-Yvon Fluorolog-3 spectrophotometer and JASCO J-851-150L CD spectrometer respectively.

Single crystal X-ray diffraction

Single crystal data for compound 1 and 2 were collected on a Bruker APEX II diffractometer equipped with a graphite monochromator and Mo-K α ($\lambda = 0.71073 \text{ \AA}$, 296 K) radiation. Data collections were performed using ϕ and ω scan. Non-hydrogen atoms are located from the difference Fourier maps, were refined anisotropically by full-matrix least-squares on F^2 , using SHELXS-97.³¹ All hydrogen atoms were included in the calculated positions and refined isotropically using a riding model. Determinations of the crystal system, orientation matrix, and cell dimensions were performed according to the established procedures. Lorentz polarization and multi-scan absorption correction were applied. All calculations were carried out using SHELXL 97,³² PLATON 99,³³ and WinGXsystemVer-1.64.³⁴

Table 1. Crystallographic refinement parameters for compounds 1 and 2.

$${}^aR_1 = \Sigma||F_o| - |F_c|| / \Sigma|F_o|, {}^bR_w = [\Sigma\{w(F_o^2 - F_c^2)^2\} / \Sigma\{w(F_o^2)^2\}]^{1/2}$$

During the final stages of refinement, some Q peaks having high electron densities were found, which probably correspond to highly disordered solvent

water molecules and are removed by SQUEEZE program.³⁴ From the TG analysis we speculate that compound **1** and **2** contains nine H₂O molecules whereas compound **3** contains six H₂O molecules and hence these are included in the molecular formula. Data collection and structure refinement parameters and crystallographic data in Table 1 and selected bond lengths and bond angles for compounds **1** and **2** are given Table S5.

Sorption measurements

Gas adsorption measurements were performed by using BelSorp-max (BEL Japan) automatic volumetric adsorption instrument. All the gases were used ultra-pure research grade (99.99%). Before every measurement samples were pretreated for 12h at 423 K under 10⁻²KPa continuous vacuum using BelPrepvac II and purged with N₂ on cooling. CO₂, CH₄ isotherms were measured at 195 K (Dry ice-MeOH cold bath). The adsorptions of different solvents like MeOH H₂O and EtOH at 298 K were measured in the vapour state by using BELSORP-aqua3 volumetric or gravimetric analyzer.

Conductivity measurements

Proton conductivity measurements of the compounds were measured by quasi-four-probe method using Solartron SI 1260 Impedance/Gain-Phase Analyzer and 1296 Dielectric Interface, in the frequency range of 1 Hz-1 MHz. For sample preparation, ~130 mg of as synthesized samples were finely grounded and then pressed in a pellet maker to obtain uniform pellets of 0.42-0.46 mm thickness, 13 mm diameter. The temperature and humidity was controlled by a programmable Incubator (JEIOTECH, TH-PE series). Samples were equilibrated for at least 8 h after each step in temperature and 12 h after each step in humidity. All the operations were computer-controlled and automatic. The resistances were calculated from the semicircles of the Nyquist plots. Proton conductivity was measured by the following equation; $\sigma = L/(R.A)$ where σ = proton conductivity, L = thickness of the pellet, R = resistance of the pellet and A = area of the pellet = $4\pi r^2$ where r = radius of the pellet. The activation energy (E_a) values were determined from the slope of Arrhenius plots by least square fitting.

Synthesis of [Cd(L-tart)(bpy)(H₂O)]_n 9n(H₂O) (1). An aqueous solution of (10 mL) L-Na₂tart of (0.3 mmol, 57 mg) was mixed with ethanol solution (12 mL) of bpy (0.3 mmol, 45 mg) and the resulting solution was stirred for 1h to mix well. Cd(NO₃)₂ 4H₂O (0.2 mmol, 60 mg) was dissolved in 15 mL of water in a separate beaker. 2 mL of the above mixed ligand solution was slowly and carefully layered above 2 mL of metal solution in a narrow glass tube using 2 mL of buffer solution (1:1 H₂O and EtOH). Colourless plate shaped single crystals were obtained from the junction of the layers after two weeks. The crystals were separated and washed with EtOH and air-

dried (Yield 80%). Elemental analysis: Cald. for C₂₈H₄₆Cd₂N₄O₂₃ (%). C, 32.6; N, 5.4; H, 4.4; Found (%): C, 32.4; N, 5.1; H, 3.9; FT-IR(KBr pellet, cm⁻¹) 3396 (b), 1670 (s),

Compound	1	2
CCDC	986614	986613
Formula	C ₂₈ H ₄₆ Cd ₂ N ₄ O ₂₃	C ₂₈ H ₄₆ Cd ₂ N ₄ O ₂₃
weight (g/mol)	1031.5	1031.5
Crystal shape	plate	plate
Color	colorless	colorless
Size	0.42×0.37×0.24	0.42×0.37×0.24
Crystal system	orthorhombic	orthorhombic
Space group	<i>P</i> 2(1)2(1)2	<i>P</i> 2(1)2(1)2
Cell length a (Å)	21.9953(12)	21.9737(11)
Cell length b (Å)	8.4064(5)	8.4037(4)
Cell length c (Å)	11.7118(7)	11.7037(6)
Cell angle alpha (°)	90.00	90.00
Cell angle beta (°)	90.00	90.00
Cell angle gamma (°)	90.00	90.00
Cell volume V (Å ³)	2165.53	2161.21
Cell formula units Z	4	4
Temperature (K)	296(2)	296(2)
λ (Mo-Kα) (Å)	0.71073	0.71073
μ (mm ⁻¹)	1.037	1.039
Dc (g cm ⁻³)	1.327	1.330
crystal_F_000	856	856
Measured reflections	6225	5504
Unique reflections	5664	4957
Goodness-of-fit	1.038	1.118
Theta range for data collection	2.54 to 29.82	2.54 to 28.51
R ₁ [I>2σ(I)] ^a	0.0422	0.0474
R _w [I>2σ(I)] ^b	0.1318	0.144

1599 (s), 1385 (s), 1112 (s), 1073 (s), 529 (b).

Synthesis of [Cd(D-tart)(bpy)(H₂O)]_n 9n(H₂O) (2).

The same diffusion technique followed for the synthesis of **2** using D-tart in place of L-tart in same 1:1:1 molar ratio using ethanol as a solvent. Colourless, plate shaped single crystals were obtained from the junction of the layers after two weeks. The crystals were separated and washed with EtOH and air-dried (Yield 73%). Elemental analysis: C₂₈H₄₆Cd₂N₄O₂₃ (%).C, 32.6; N, 5.4; H, 4.4; Found (%): C, 32.4; N, 5.1; H, 3.9; FT-IR (KBr pellet, cm⁻¹) 3376 (b), 1670 (s), 1605 (s), 1385 (s), 1112 (s), 1066 (s), 633 (b).

Synthesis of [Cd(D-tart)(L-tart)(bipy)(H₂O)]_n 7n(H₂O) (3).

The same diffusion technique followed for the synthesis of **3** using DL-tart in place of L-tart in same 1:1:1 molar ratio using ethanol as a solvent. Colourless crystalline compounds were obtained from the junction of the layers after two weeks. The crystals were separated and washed with EtOH and air-dried (Yield 45%). Elemental analysis: Anal. Cald. for

C28H40Cd2N4O20 (%). C, 34.4; N, 5.7; H, 4.1; Found (%): C, 34.1; N, 5.2; H, 3.5; FT-IR (KBr pellet, cm^{-1}) 3376 (b), 1667 (s), 1612 (s), 1392 (s), 1112 (s), 1066 (s), 646 (b).

ACKNOWLEDGMENT

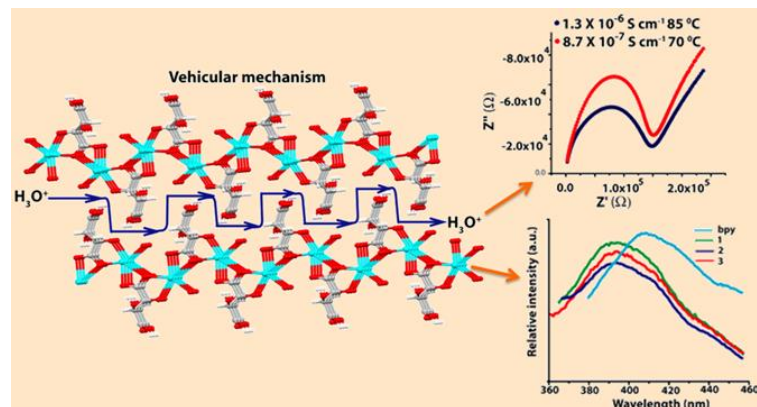
SP, SS thank IISER Bhopal for the PhD fellowships and HSJ thanks for post-doctoral fellowship. S.K. thanks CSIR, Government of India (Project No.01/(2473)/11/EMRII), and IISER Bhopal for generous financial and infrastructural support. Authors sincerely thank to Dr. H. N. Gopi, IISER Pune, for CD measurements.

REFERENCES

- (a) M. Kondo, T. Yoshitomi, K. Seki, H. Matsuzaka and S. Kitagawa, *Angew. Chem., Int. Ed.*, 1997, **36**, 1725; (b) J. L. C. Rowsell and O. M. Yaghi, *Angew. Chem., Int. Ed.*, 2005, **44**, 4670; (c) B. D. Chandler, G. D. Enright, K. A. Udachin, S. Pawsey, J. A. Ripmeester, D. T. Cramb and G. K. H. Shimizu, *Nat. Mater.*, 2008, **7**, 229; (d) S. A. Dalrymple and G. K. H. Shimizu, *J. Am. Chem. Soc.*, 2007, **129**, 121141; (e) T. A. Makal, J. R. Li, W. Lu and H.-C. Zhou, *Chem. Soc. Rev.*, 2012, **41**, 7761; (f) J. R. Li, R. J. Kuppler and H.-C. Zhou, *Chem. Soc. Rev.*, 2009, **38**, 1477; (g) M. Eddaoudi, J. Kim, N. Rosi, D. Vodak, J. Wachter, M. O'Keeffe and O. M. Yaghi, *Science* 2002, **295**, 469; (h) H. Hayashi, A. P. Coté, H. Furukawa, M. O'Keeffe and O. M. Yaghi, *Nat. Mater.*, 2007, **6**, 501; (i) S. Parshamoni, S. Sanda, H. S. Jena, and S. Konar, *Dalton Trans.*, 2014, **43**, 7191; (j) S. Biswas, H. S. Jena, S. Goswami, S. Sanda and S. Konar, *Cryst. Growth Des.*, 2014, **14**, 1287.
- (a) G. Ferey, F. Millange, M. Morcrette, C. Serre, M. L. Doublet, J. M. Greneche and J. M. Tarascon, *Angew. Chem., Int. Ed.*, 2007, **46**, 3259; (b) S. Ohkoshi, K. Nakagawa, K. Tomono, K. Imoto, Y. Tsunobuchi and H. Tokoro, *J. Am. Chem. Soc.*, 2010, **132**, 6620; (c) J. A. Hurd, R. Vaidhyanathan, V. Thangadurai, C. I. Ratcliffe, I. M. Moudrakovski and G. K. H. Shimizu, *Nat. Chem.*, 2009, **1**, 705; (d) C. Y. Duan, M. L. Wei, D. Guo, C. He and Q. J. Meng, *J. Am. Chem. Soc.*, 2010, **132**, 3321; (e) S. C. Sahoo, T. Kundu and R. Banerjee, *J. Am. Chem. Soc.*, 2011, **133**, 17950; (f) S. Bureekaew, S. Horike, M. Higuchi, M. Mizuno, T. Kawamura, D. Tanaka, N. Yanai and S. Kitagawa, *Nat. Mater.*, 2009, **8**, 831; (g) D. Umeyama, S. Horike, M. Inukai, Y. Hijikata and S. Kitagawa, *Angew. Chem., Int. Ed.*, 2011, **50**, 1; (h) N. C. Jeong, B. Samanta, C. Y. Lee, O. K. Farha and J. T. Hupp, *J. Am. Chem. Soc.*, 2012, **134**, 51;
- (a) Y.-G. Sun, X. -F. Gu, F. Ding, P. F. Smet, E. -J. Gao, D. Poelman and F. Verpoort, *Cryst. Growth Des.*, 2010, **10**, 1059; (b) X.-J. Wang, Z. -M. Cen, Q. -L. Ni, X. -F. Jiang, H. -C. Lian, L. -C. Gui, H.-H. Zuo and Z. -Y. Wang, *Cryst. Growth Des.*, 2010, **10**, 2960; (c) H.-B. Xu, X. -M. Chen, Q. -S. Zhang, L. -Y. Zhang and Z. -N. Chen, *Chem. Commun.*, 2009, 7318; (d) S. Sanda, S. Parshamoni, A. Adhikary and S. Konar, *Cryst. Growth Des.*, 2013, **13**, 5442.
- (a) A. Corma, H. Garcia and F. X. Llabres i Xamena, *Chem. Rev.*, 2010, **110**, 4606; (b) J. Y. Lee, O. K. Farha, J. Roberts, K. A. Scheidt, S. T. Nguyen and J. T. Hupp, *Chem. Soc. Rev.* 2009, **38**, 1450; (c) M. Fujita, Y. J. Kwon, S. Washizu and K. Ogura, *J. Am. Chem. Soc.*, 1994, **116**, 1151; (d) C. D. Wu, A. Hu, L. Zhang and W. Lin, *J. Am. Chem. Soc.* 2005, **127**, 8940; (e) Z. Q. Wang and S. M. Cohen, *Chem. Soc. Rev.*, 2009, **38**, 1315.
- (a) J. S. Seo, D. Whang, H. Lee, S. I. Jun, J. Oh, Y. J. Jeon and K. Kim, *Nature* 2000, **404**, 982; (b) K. Nomiya, S. Takahashi, R. Noguchi, S. Nemoto, T. Takayama and M. Oda, *Inorg. Chem.*, 2000, **39**, 3301; (c) L. Ma, C. Abney and W. Lin, *Chem. Soc. Rev.*, 2009, **38**, 1248; (d) R. E. Morris and X. Bu, *Nat. Chem.*, 2010, **2**, 353.
- (a) G. Li, W. Yu and Y. Cui, *J. Am. Chem. Soc.*, 2008, **130**, 4582; (b) M. C. Das, Q. S. Guo, Y. B. He, J. Kim, C. G. Zhao, K. L. Hong, S. C. Xiang, Z. T. Zhang, K. M. Thomas, R. Krishna and B. L. Chen, *J. Am. Chem. Soc.*, 2012, **134**, 8703; (c) K. K. Bisht and E. Suresh, *J. Am. Chem. Soc.*, 2013, **135**, 15690.
- (a) X. Duan, Q. Meng, Y. Su, Y. Li, C. Duan, X. Ren and C. Lu, *Chem. Eur. J.*, 2011, **17**, 9936; (b) O. R. Evans and W. Lin, *Acc. Chem. Res.* 2002, **35**, 511; (c) C. Wang, T. Zhang and W. Lin, *Chem. Rev.*, 2012, **112**, 1084.
- (a) K. K. Bisht and E. Suresh, *Inorg. Chem.* 2012, **51**, 9577; (b) L. Pérez-García and D. B. Amabilino, *Chem. Soc. Rev.*, 2002, **31**, 342; (c) Q. -Y. Liu, Y. -L. Wang, N. Zhang, Y. -L. Jiang, J. -J. Wei and F. Luo, *Cryst. Growth Des.*, 2011, **11**, 3717; (d) E. -Q. Gao, Y. -F. Yue, S. -Q. Bai, Z. He, and C. -H. Yan, *J. Am. Chem. Soc.*, 2004, **126**, 1419; (e) X. -L. Tong, T. -L. Hu, L. -P. Zhao, Y. -K. Wang, H. Zhang and X. -H. Bu, *Chem. Commun.*, 2010, **46**, 8543.
- (a) L. Ma, J. M. Falkowski, C. Abney and W. B. Lin, *Nat. Chem.*, 2010, **2**, 838; (b) F. J. Song, C. Wang, J. M. Falkowski, L. Q. Ma and W. B. Lin, *J. Am. Chem. Soc.*, 2010, **132**, 15390; (c) R. Vaidhyanathan, D. Bradshaw, J. -N. Rebilly, J. P. Barrio, J. A. Gould, N. G. Berry and M. J. Rosseinsky, *Angew. Chem., Int. Ed.*, 2006, **45**, 6495; (d) K. Suh, M. P. Yutkin, D. N. Dybtsev, V. P. Fedinc and K. Kim, *Chem. Commun.*, 2012, **48**, 513.
- (a) S. K. Ghosh, J. Ribas and P. K. Bharadwaj, *Cryst. Growth Design.*, 2005, **5**, 623; (b) J. -C. Dai, X. -T. Wu, Z. -Y. Fu, S. -M. Hu, W. -X. Du, C. -P. Cui, L. -M. Wu, H. -H. Zhang and R. -Q. Sun, *Chem. Commun.*, 2002, 12; (c) D. Sun, R. Cao, Y. Liang, Q. Shi, W. Su and M. J. Hong, *Chem. Soc., Dalton Trans.*, 2001, 2335; (d) C. S. Hong, S. K. Son, Y. S. Lee, M. J. Jun and Y. Do, *Inorg. Chem.*, 1999, **38**, 5602.
- (a) K. D. Kreuer, S. J. Paddison, E. Spohr and M. Schuster, *Chem. Rev.*, 2004, **104**, 4637; (b) B. C. Steele and A. Heinzl, *Nature* 2001, **414**, 345.
- K. A. Marutz and R. B. Moore, *Chem. Rev.*, 2000, **104**, 4535.
- N. G. Hainovsky, Y. T. Pavlukhin and E. F. Hairetdinov, *Solid State Ionics* 1986, **20**, 249.
- (a) M. Sadakiyo, H. Ōkawa, A. Shigematsu, M. Ohba, T. Yamada and H. Kitagawa, *J. Am. Chem. Soc.*, 2012, **134**, 5472; (b) S. Ohkoshi, K. Nakagawa, K. Tomono, K. Imoto, Y. Tsunobuchi and H. Tokoro, *J. Am. Chem. Soc.*, 2010, **132**, 6620; (c) D. Umeyama, S. Horike, M. Inukai, Y. Hijikata and S. Kitagawa, *Angew. Chem., Int. Ed.*, 2011, **50**, 1; (d) Y. Nagao, R. Ikeda, S. Kanda, Y. Kubozono and H. Kitagawa, *Mol. Cryst. Liq. Cryst.*, 2002, **379**, 89; (e) J. A. Hurd, R. Vaidhyanathan, V. Thangadurai, C. I. Ratcliffe, I. M. Moudrakovski and G. K. H. Shimizu, *Nat. Chem.*, 2009, **1**, 705; (f) J. M. Taylor, R. K. Mah, I. L. Moudrakovski, C. I. Ratcliffe, R. Vaidhyanathan and G. K. H. Shimizu, *J. Am. Chem. Soc.*, 2010, **132**, 14055; (g) S. Bureekaew, S. Horike, M. Higuchi, M. Mizuno, T. Kawamura, D. Tanaka, N. Yanai and S. Kitagawa, *Nat. Mater.*, 2009, **8**, 831; (h) H.

- Okawa, M. Sadakiyo, T. Yamada, M. Maesato, M. Ohba and H. Kitagawa, *J. Am. Chem. Soc.*, 2013, **135**, 2256; (i) M. Sadakiyo, T. Yamada and H. Kitagawa, *J. Am. Chem. Soc.*, 2009, **131**, 9906.
15. (a) Y. Kobayashi, B. Jacobs, M. D. Allendorf and J. R. Long, *Chem. Mater.*, 2010, **22**, 4120; (b) M. Sadakiyo, T. Yamada and H. Kitagawa, *J. Am. Chem. Soc.*, 2009, **131**, 9906; (c) J. A. Hurd, R. Vaidyanathan, V. Thangadurai, C. Ractcliffe, I. L. Moudrakovski, G. K. H. Shimizu, *Nat. Chem.*, 2009, **1**, 705; (d) S. Brueckewald, S. Horike, M. Higuchi, M. Mizuno, T. Kawamura, D. Tanaka, N. Yanai and S. Kitagawa, *Nat. Mater.*, 2009, **8**, 831.
 16. (a) F. Costantino, A. Donnadio and M. Casciola, *Inorg. Chem.*, 2012, **51**, 6992; (b) S. R. Kim, K. W. Dawson, B. S. Gelfand, J. M. Taylor and G. K. H. Shimizu, *J. Am. Chem. Soc.*, 2013, **135**, 963; (c) J. M. Taylor, K. W. Dawson and G. K. H. Shimizu, *J. Am. Chem. Soc.*, 2013, **135**, 1193; (d) A. Shigematsu, T. Yamada and H. Kitagawa, *J. Am. Chem. Soc.*, 2011, **133**, 2034; (e) A. Mallick, T. Kundu and R. Banerjee, *Chem. Commun.* 2012, **48**, 8829.
 17. (a) S. C. Sahoo, T. Kundu and R. Banerjee, *J. Am. Chem. Soc.*, 2011, **133**, 17950; (b) E. Pardo, C. Train, G. Gontard, K. Boubekeur, O. Fabelo, H. Liu, B. Dkhil, F. Lloret, K. Nakagawa, H. Tokoro, S. Ohkoshi and M. Verdager, *J. Am. Chem. Soc.*, 2011, **133**, 15328.
 18. R. M. P. Colodrero, K. E. Papathanasiou, N. Stavgiannoudaki, P. Olivera-Pastor, E. R. Losilla, M. A. G. Aranda, L. Leon-Reina, J. Sanz, I. Sobrados, D. Choquesillo-Lazarte, J. M. Garcia-Ruiz, P. Atienzar, F. Rey, K. D. Demadis and A. Cabeza, *Chem. Mater.*, 2012, **24**, 3780.
 19. E. Coronado, J. R. Galán-Mascarós, C. J. Gómez-García Prof. and A. Murcia-Martínez, *Chem.–Eur. J.*, 2006, **12**, 3484.
 20. S. Parshamoni, S. Sanda, H. S. Jena, K. Tomar and S. Konar, *Cryst. Growth Des.*, 2014, **14**, 2022.
 21. (a) R. A. Coxall, S. G. Harris, D. K. Henderson, S. Parsons, P. A. Tasker and R. E. P. Winpenny, *J. Chem. Soc., Dalton Trans.*, 2000, 2349; (b) S. Khatua, S. Goswami, S. Parshamoni, H. S. Jena and S. Konar, *RSC Adv.*, 2013, **3**, 25237.
 22. V. A. Blatov, A. P. Shevchenko and V. N. Serezhkin, TOPOS3.2: a new version of the program package for multipurpose crystal–chemical analysis, *J. Appl. Crystallogr.*, 2000, **33**, 1193.
 23. K. L. Gurunatha and T. K. Maji, *Inorg. Chim. Acta* 2009, **362**, 1541; (b) A. Hazra, P. Kanoo, S. Mohapatra, G. Mostafa and T. K. Maji, *CrystEngComm.*, 2010, **12**, 2775.
 24. (a) J. Kumar, P. Kanoo, T. K. Maji and S. Verma, *CrystEngComm.*, 2012, **14**, 3012; (b) S. Sanda.; S. Goswami.; H. S. Jena.; S. Parshamoni and S. Konar. *CrystEngComm.*, 2014,**16**, 4742-4752.
 25. P. Kanoo, G. Mostafa, R. Matsuda, S. Kitagawa and T. K. Maji, *Chem. Commun.*, 2011, **47**, 8106; (b) S. Sanda, S. Parshamoni and S. Konar, *Inorg. Chem.*, 2013, **52**, 12866.
 26. (a) V. V. Brus, *SEMICONDUCTORS.*, 2012, **46**, 1012, (b) V. V. Brus, *Semicond. Sci. Technol.*, 2012, **27**, 035024, (c). V.V. Brus, M. Zellmeier, X. Zhang, S.M. Greil, M. Gluba, A.J. Töfflinger, J. Rappich, N.H. Nickel, *Organic Electronics* 2013, **14**, 3109.
 27. (a) M. Yoon, K. Suh, S. Natarajan and K. Kim, *Angew. Chem., Int. Ed.*, 2013, **52**, 2688; (b) J. A. Hurd, R. Vaidyanathan, V. Thangadurai, C. I. Ratcliffe, I. L. Moudrakovski and G. K. H. Shimizu, *Nature Chem.*, 2009, **1**, 705; (c) N. C. Jeong, B. Samanta, C. Y. Lee, O. K. Farha and J. T. Hupp, *J. Am. Chem. Soc.*, 2011, **134**, 51; (d) T. Yamada, M. Sadakiyo and H. Kitagawa, *J. Am. Chem. Soc.*, 2009, **131**, 3144.
 28. (a) X. Y. Dong, R. Wang, J. B. Li, S. Q. Zang, H. W. Hou and T. C. W. Mak, *Chem. Commun.*, 2013, **49**, 1059; (b) K. -D. Kreuer, *Chem. Mater.*, 1996, **8**, 610; (c) K. D. Kreuer, A. Rabenau, R. Messer, *Appl. Phys. A: Mater. Sci. Process.*, 1983, **32**, 45; (d) A. Telfah, G. Majer, K. D. Kreuer, M. Schuster and Maier, *J. Solid State Ionics* 2010, **181**, 461.
 29. (a) W. Yang, F. Yi, X. Li, L. Wang, S. Dang and Z. Sun, *RSC Adv.*, 2013, **3**, 25065; (b) H. Wang, F. Yi, S. Dang, W. Tian and Z. Sun, *Cryst. Growth Des.*, 2014, **14**, 147; (c) R. B. Fu, S. C. Xiang, S. M. Hu, L. S. Wang, Y. M. Li, X. H. Huang and X. T. Wu, *Chem. Commun.*, 2005, 5292; (d) X. D. Guo, G. S. Zhu, Q. R. Fang, M. Xue, G. Tian, J. Y. Sun, X. T. Li and S. L. Qiu, *Inorg. Chem.*, 2005, **44**, 3850; (e) J. Zhang, W. Lin, Z. F. Chen, R. G. Xiong, B. F. Abrahams and H. K. Fun, *Dalton Trans.*, 2001, 1806; (d) C. D. Wu, H. L. Ngo and W. Lin, *Chem. Commun.*, 2004, 1588.
 30. (a) L. Y. Zhang, J. P. Zhang, Y. Y. Lin and X. M. Chen, *Cryst. Growth Des.*, 2006, **6**, 1684; (b) D. Niu, J. Yang, J. Guo, W. Kan, Q. S. Y. Song, P. Du and J. F. Ma, *Cryst. Growth Des.*, 2012, **12**, 2397; (c) X. L. Wang, C. Qin, E. B. Wang, Y. G. Li, N. Hao, C. W. Hu and A. L. Xu, *Inorg. Chem.*, 2004, **43**, 1850; (d) J. -H. Yang, W. Li, S. -L. Zheng, Z. -L. Huang and X. -M. Chen, *Aust. J. Chem.*, 2003, **56**, 1175; (e) S. -L. Zheng, J. -M. Yang, X. -L. Yu, X.-M. Chen, W. -T. Wong, *Inorg. Chem.*, 2004, **43**, 830.
 31. G. M. Sheldrick, SHELXTL Program for the Solution of Crystal of Structures, University of Göttingen, Göttingen, Germany, 1993.
 32. G. M. Sheldrick, SHELXL 97, Program for Crystal Structure Refinement, University of Göttingen, Göttingen, Germany, 1997.
 33. A. L. Spek, *J. Appl. Crystallogr.*, 2003, **36**, 7.
 34. L. J. Farrugia, *J. Appl. Crystallogr.*, 1999, **32**, 837.

Table of Contents



We report three Cd(II) based H-bonded 3D MOFs formed by the hydrogen bonded interaction between the nearby 2D pillared-layer framework. All the compounds show significant amount of uptake for water vapor over other organic solvents and an Impedance measurement indicates their show proton conductivity at higher temperature (358 K) at 95% relative humidity. The photoluminescence properties of all the compounds are also reported